Static Signature Synthesis: A Neuromotor Inspired Approach for Biometrics

Miguel A. Ferrer, Moises Diaz-Cabrera and Aythami Morales

Abstract—In this paper we propose a new method for generating synthetic handwritten signature images for biometric applications. The procedures we introduce imitate the mechanism of motor equivalence which divides human handwriting into two steps: the working out of an effector independent action plan and its execution via the corresponding neuromuscular path. The action plan is represented as a trajectory on a spatial grid. This contains both the signature text and its flourish, if there is one. The neuromuscular path is simulated by applying a kinematic Kaiser filter to the trajectory plan. The length of the filter depends on the pen speed which is generated using a scalar version of the sigma lognormal model. An ink deposition model, applied pixel by pixel to the pen trajectory, provides realistic static signature images. The lexical and morphological properties of the synthesized signatures as well as the range of the synthesis parameters have been estimated from real databases of real signatures such as the MCYT Off-line and the GPDS960GraySignature corpuses. The performance experiments show that by tuning only four parameters it is possible to generate synthetic identities with different stability and forgers with different skills. Therefore it is possible to create datasets of synthetic signatures with a performance similar to databases of real signatures. Moreover, we can customize the created dataset to produce skilled forgeries or simple forgeries which are easier to detect, depending on what the researcher needs. Perceptual evaluation gives an average confusion of 44.06% between real and synthetic signatures which shows the realism of the synthetic ones. The utility of the synthesized signatures is demonstrated by studying the influence of the pen type and number of users on an automatic signature verifier.

Index Terms—Biometric recognition, off-line signature verification, synthetic generation, motor equivalence theory, kinematic theory of human movements, ink deposition model.

1 Introduction

THE use of biometric traits has become well-established in commerce and forensics [1]. The most commonly used traits for identification or verification are the face [2], the fingerprint [3] and the iris [4]. Among the most challenging biometrics are those related to human behavior because of their unpredictable variability. It is well-established that during the early stages of development the human neuromotor system learns a way of writing, walking, key stroking, etc. that contains a sort of 'water mark' for the person's identity. This water mark is difficult to imitate or disguise by a forger because of the differences between individuals' neuromuscular systems. This therefore gives a theoretical advantage to these behavioral biometrics. It is, however, enormously difficult to detect and characterize this water mark. This is because of both the relatively few samples generally available and the inherent variability of human behavior. This can change not only for psychological reasons but also because of the adaptation of different postures, the wearing of different dress, the use of different writing tools and for other unaccountable factors.

In a behavioral biometric such as the handwritten signature, research nowadays tends to focus on improving recognition accuracy, although topics such as interoperability, standards, scalability and template protection are also gaining attention. Obtaining statistically reliable performance evaluation is not only time consuming and expensive but also requires the availability of large databases and common benchmarks. Well-established experimental protocols and benchmarks alleviate some of the drawbacks in performance evaluation. Several standards [5], procedures [6], databases (e.g. [7][8][9][10]) and competitions (e.g. [11]) have been developed for this purpose. Additionally, legal issues regarding data protection hamper the sharing and distribution of biometric data [1][12].

The use of synthetic biometric data in large datasets has recently emerged as an aid to more accurate performance evaluation. Such data has been applied to fingerprints [11], faces [13], the iris [14], speech [15], handwriting [16] and even signatures [17][18][19][20]. These datasets can improve the assessment of vulnerability and algorithm robustness. Legal considerations are, of course, paramount.

The proposals in the literature for synthetic handwritten signatures are as follows [19]:

Generation of duplicated samples. The synthesis algorithm generates new samples from those of an existing user. The generator produces new duplicates through several transformations. An example of dynamic signature duplication can be found in [21] for improving enrollment in dynamic signature verification. In [18] new static signatures are generated from two dynamic samples produced by the same user. The GAVAB static handwritten signature database comprises signatures duplicated by affine transformation of the original signatures [8].

• *All Authors are with the Instituto Universitario para el Desarrollo Tecnológico y la Innovación en Comunicaciones, Universidad de Las Palmas de Gran Canaria, Las Palmas, 35017, Spain. E-mail: {mferrer, mdiaz, amorales}@idetic.eu.*

xxxx-xxxx/0x/$xx.00 © 200x IEEE Published by the IEEE Computer Society

This article has been accepted for publication in a future issue of this journal, but has not been fully edited. Content may change prior to final publication. Citation information: DOI 10.1109/TPAMI.2014.2343981, IEEE Transactions on Pattern Analysis and Machine Intelligence

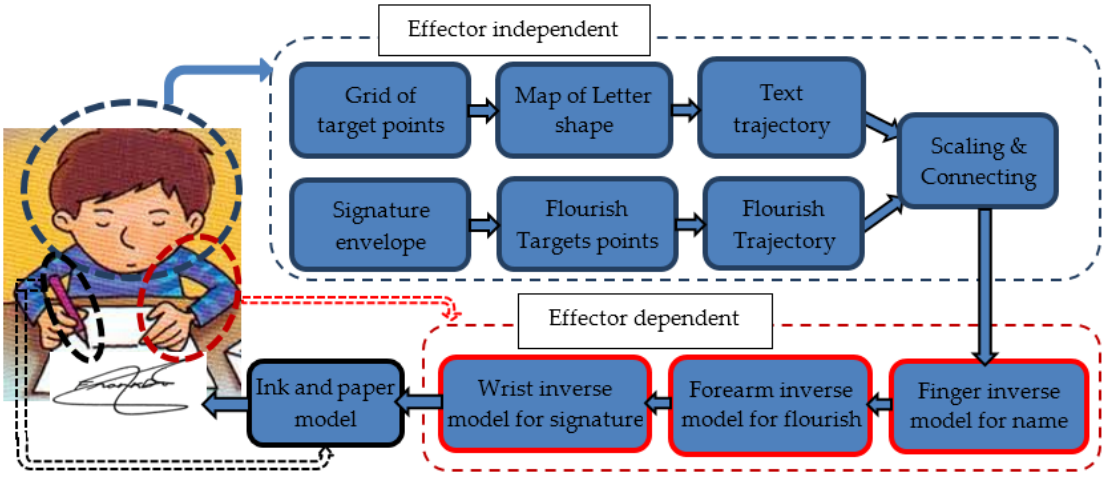

Fig. 1. Motor equivalence approach to synthetic off-line signature generation.

Generation of new synthetic identities. Here, the new signers and their signatures are created from statistical descriptors. Although there are several handwriting synthesizers in the literature, few synthesize samples for a new identity. Popel in [17] describes an approach for signature generation using a model based on visual characteristics extracted from the time domain. After a visual validation, no clear quantitative results are given. A novel methodology is proposed by Galbally et al. in [19][20] for the generation of synthetic on-line signatures on the basis of flourish and isolated characters. Their method combines the advantages of both spectral analysis and the kinematic theory of rapid human movements to generate the master signature of a new identity. Similarly, a proposal to use heuristic procedures to generate genuine and forged signatures is proposed at [21].

Recognizing that signing is a human task which involves complex cognitive functions and fine motor control, this paper proposes a novel method of generating both genuine and forged signatures of new synthetic identities. This is performed by attempting to emulate the mechanism of motor equivalence which is defined as the personal ability to perform the same movement pattern by different muscles.

The motor equivalence theory, also known as the Degrees of Freedom (DoF) problem, it was formulated by K. Lashley [22] and it was N. Bernstein who articulated it in its current form [23]. Their studies are based on the activity of the Central Nervous System (CNS) which controls posture and movement and focus on the kinematical properties, seen from a musculo-skeletal viewpoint.

The motor equivalence theory suggests that the brain stores in two steps the movements aimed at performing a single task. The first is called effector-independent which stores the movement in an abstract form as a spatial sequence of points representing the action plan. The parietal cortex in general, and the posterior parietal cortex and the occipitotemporal junction in particular, are suggested in [24] as the most important brain region for representation of the action plan. The second step is called effector dependent and consist of a sequence of motor commands directed at obtaining particular muscular contractions and articulatory movements in order to execute the action plan [25] .

Applying the equivalence model to handwriting, the action plan may be represented in terms of strokes which are encoded in terms of relative positions and spatial directions. Once the movement has been planned, the motor control delivers the commands to specific muscles to produce the handwriting.

In [26] it is suggested that fast and coordinated movements cannot be executed solely under feedback control since biological feedback is slow. Thus [26] proposes that the brain needs to acquire an inverse model of the object to be controlled by motor learning. Focusing on the internal inverse model of the limbs created by the cerebellum, [26] calculates the motor commands which compensate for the arm's dynamics. Therefore, in the human development stage, early handwriting actions are highly demanding of attention, slow to execute, clumsy and not particularly accurate. After long-term practice, the movements become quick, smooth, automatic, and can be performed effortlessly, using minimal cognitive resources. This all suggests that the internal model could be replicated by a kinematic filter.

The kinematic filter is designed based on the kinematic theory which describes a stroke velocity profile as the output of a system made of two neuromuscular systems: one, an agonist, acting in the direction of the movement, and the other, an antagonist, acting in the opposite direction, compensating for the arm dynamics or inertia. The composition of the agonist, antagonist and arm inertia produce the well-known stroke overlapping which conveys handwritten quadratic trajectories [27][28][29][30].

Using motor equivalence, the inverse model and kinematic theory, we propose an off-line handwritten signature synthesizer. Obviously, we do not pretend to model the mechanism of motor equivalence. Our idea is to construct a synthetic signature generator, inspired by motor equivalence hypotheses, which is built as follows (see Fig.

This article has been accepted for publication in a future issue of this journal, but has not been fully edited. Content may change prior to final publication. Citation information: DOI 10.1109/TPAMI.2014.2343981, IEEE Transactions on Pattern Analysis and Machine Intelligence

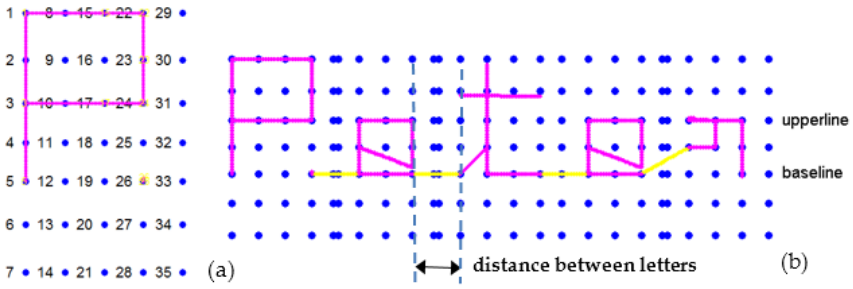

Fig. 2. (a) Grid of trajectory points with their labels of the letter trajectory plan for letter 'P'; (b) Text trajectory plan for 'Peter' obtained by concatenating the letter trajectory plans. The text trajectory plan is depicted in dark magenta and the link plan between letters in yellow.

1): Firstly, we define the signature trajectory plan, which imitates the action plan; Secondly, we use an approach to the inverse internal models based on kinematic filters. Thirdly, given a synthetic identity, we propose a model of within and between individuals for constructing different signature samples and a method for generating forgeries at different skill levels. To the best of our knowledge, this is the first work which deals with the generation of realistic synthetic genuine and synthetic forged signatures each of which may contain text and a flourish, if there is one. A particular merit of our proposal is the possibility of controlling the synthesized identity's stability and the synthesized forger's skill by tuning no more than four parameters. All the constants and parameters of the proposed model are worked out from the statistical distribution of global and local properties from the signatures in well-known public databases, such as the MCYT Off-line and GPDS960GRAYsignature. An ink deposition model is used for creating realistic static signature images.

The aims of our experiments are: firstly, to determine the ability, in terms of the equal error rate, of the synthesizer to generate identities with different stability and forgers with different skills; and secondly to be able to assess the realism of the generated images by a perceptual survey. Furthermore, a synthetic database of 4000 synthetic signers with 24 genuine samples and 30 forgeries with different inks is generated and made publicly available at http://www.gpds.ulpgc.es/download. This database is obviously free of any legal concerns on privacy.

The paper is presented as follows: sections 2 and 3 respectively describe the trajectory plan and the inverse motor approaches. Section 4 is devoted to the ink model. Section 5 is dedicated to the signature synthesizer parameters. Section 6 is focused on the performance and perceptual experiments while section 7 shows a case study of the usefulness of the signature synthesizer. The eighth section closes the paper with conclusions and suggested future research.

2 Synthetic Signature Trajectory Plan

This section proposes a trajectory plan which imitates the cognitive action plan for a handwritten signature. During the early development stage, human beings learn in visual coordinates the spatial sequence associated with the motor task [24] of generating a signature. Firstly, the sequence of points needed to generate the inked trace is learned. Then, the sequence of motor commands is acquired and executed as a single action.

We assume the Western style of signing, which is either one of or a combination of a text and a flourish. The proposed trajectory plan is described in two steps: text trajectory and flourish trajectory. If both exist, once defined, they are scaled and connected. The method allows the generation of several types of signatures with different complexity levels.

2.1 Text Trajectory Plan

Learning to write is a complex procedure which starts with lines and scribbles. After reaching the age of about 3 years, most children understand that writing is made by combining lines, curves, and repeated patterns. About a year later, children begin to use letters in their own style. Usually they start by experimenting with the letters in their own names, as these are the letters most familiar to them. Thus, children begin to learn the shape and sequence of the letters in their name although their motor control is not yet accurate.

In some countries, children start their handwriting practice using printed worksheets. These help them to guide the height, width and length of each alphabetical letter they write or trace, whether in upper or lower case, and to construct the numerals. The tracing of lines or the joining up of dots, within the lines on a worksheet, helps them to learn each letter shape and the writing sequence. The lines help the formation of spatial relationships between objects thus creating the spatial memory or cognitive map. Once this is acquired, a child is able to select an ordered sequence of target points to perform fluent writing.

The cognitive map of the writing sequence is imitated in this paper by a letter trajectory plan which consists of: i) a grid of possible trajectory points, distributed in the signing area, which simulates the cognitive map; and ii) a set of letter trajectory plans which describe the sequence of trajectory points necessary to write each letter. The text trajectory plan is built by concatenating horizontally the letter trajectory plan of each letter with the necessary horizontal spaces between them.

This article has been accepted for publication in a future issue of this journal, but has not been fully edited. Content may change prior to final publication. Citation information: DOI 10.1109/TPAMI.2014.2343981, IEEE Transactions on Pattern Analysis and Machine Intelligence

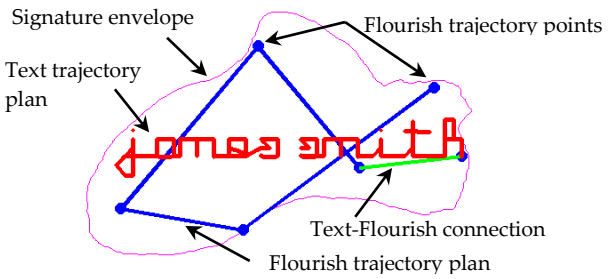

Fig. 3. Signature envelope, text and flourish trajectory plan of "james smith".

The grid of trajectory points for each letter is shown in Fig. 2. Each point is labeled with a number. The distance between columns and rows of the grid define the letter shape and writing style which is generally different for different writers but constant for each writer.

For each letter, the trajectory plan is defined as a sequence of trajectory points. For instance, the trajectory plan for the letter 'P' is defined as the following sequence of trajectory points: {5, 1, 8, 15, 22, 23, 24, 17, 10, 3}. For the letter 'e' it is {11, 18, 25, 24, 17, 10, 11, 12, 19, 26} and so on. The result can be seen in Fig. 2 . The trajectory points in which the pen should stop because the writer has lifted the pen from the paper (for instance to write the upper horizontal line in the letter 't' or because of a discontinuity or a pen direction change) are marked as the initial point of a new stroke. Note that these trajectory points are not necessarily related with the so called target point in the cortex action plan. This procedure to synthesize off-line signatures is loosely based on the motor equivalence model theory but it does not pretend to model or simulate it.

Finally, the trajectory plan of a given text is defined by concatenating the trajectory plan of different letters, as in Fig. 2. The distance between letters is related to the grid size and defined later, although it appears constant in Fig. 2.

2.2 Flourish Trajectory Plan

The flourish trajectory points are defined as a sequence of points randomly generated inside a synthetic signature envelope. This envelope attempts to imitate the signing area that often limits the flourish area in the user brain.

The signature envelope is modeled by means of an Active Shape Model (ASM) which consist of a mean signature shape $\bar{x}$, a matrix P of eigenvectors which describe the main modes of variation of the envelope and a vector b of weights [31][32]. The ASM is trained according the methodology proposed in [31] with the MCYT off-line database.

A new synthetic signature envelope is obtained as $x^f = \bar{x} + P \cdot b$. This is calculated by selecting the b vector weights randomly from within a uniform distribution of mean zero and deviation equal to $|b_k| < 4\sqrt{\lambda_k}$, where λ_k are the eigenvalues of the P matrix eigenvectors.

The flourish trajectory points are located randomly inside the signature contour. The number of target points is constant for a given user. As the signature envelope contains the signature, the flourish trajectory points are randomly located as separately as possible, taking into account that the line joining the consecutive trajectory points does not cross the envelope. An example is shown in Fig. 3.

If there are both a text and a flourish, their trajectory plans are combined in three steps. The first displaces the geometrical center of the text trajectory plan to the mass center of the signature envelope. The second resizes the text trajectory plan to adjust the scale between both trajectory plans. The scale is the ratio between the text length and the horizontal contour width. The value for the scale is an identity constant. In the third step, the signature trajectory plan is obtained by concatenating the text and flourish trajectory plan adding, if the text and flourish are connected, a link between the end of the text trajectory plan and the beginning of the flourish trajectory plan. An example where both trajectory plans are connected can be seen in Fig. 3.

3 Motor Control Approach

Once the signature trajectory plan is defined, an inverse model for motor control is applied to obtain a realistic human signature trajectory. Theories on how the arm reaches planned trajectories are a central issue in motor control. The strokes are considered as primitives from which complex movements are assumed to be planned and executed. The strokes reflect some of the fundamental properties of a writer's neuromuscular system, as well as some of the basic features of the motor control strategies employed to produce these simple movements. Among these basic features, the most remarkable is the invariance of the velocity profile of the end-effector for a subject performing a rapid stroke over a wide range of movement size and speed [33]. Many of the different computational models can be classified into two main types: kinematic and dynamic. The kinematic model has been found to be successful in reproducing the various invariants observed in rapid strokes.

The kinematic theory describes a stroke velocity profile as the output of a system made of two neuromuscular systems: one, an agonist, acting in the direction of the movement, and other, an antagonist, acting in the opposite direction, compensating for the arm dynamics or inertia. The composition of the agonist, antagonist and arm inertia produce the well-known stroke overlapping which convey handwritten quadratic trajectories. The kinematic theory models the velocity of both movements by a Delta-lognormal. Each lognormal is characterized by its amplitude D, time of occurrence τ, the log time delays μ and the log-response time σ. The velocity profile of a stroke is then:

$$v^t = D_1 \Lambda(t; \tau_1, \mu_1, \sigma_1^2) - D_2 \Lambda(t; \tau_2, \mu_2, \sigma_2^2) \quad (1)$$

where

$$\Lambda(t; \tau, \mu, \sigma^2) = \frac{1}{\sigma\sqrt{2\pi}(t-\tau)} exp\left\{-\frac{[\ln(t-\tau)-\mu]^2}{2\sigma^2}\right\}$$

for $t > \tau$, and 0 elsewhere.

Introducing the kinematic model within the trajectory plan will convert the sequence of straight lines into a

This article has been accepted for publication in a future issue of this journal, but has not been fully edited. Content may change prior to final publication. Citation information: DOI 10.1109/TPAMI.2014.2343981, IEEE Transactions on Pattern Analysis and Machine Intelligence

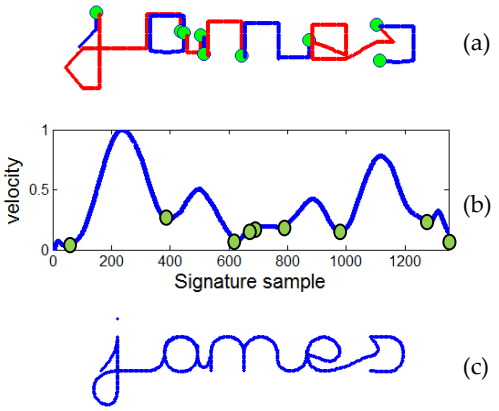

Fig. 4. a) Trajectory plan of letters "james" with stroke division marked with a circle and each consecutive stroke with change in color; b) Velocity profile v_f^t based on scalar Sigma lognormal normalized to maximum amplitude equal to one; and c) The resulting handwriting word after applying the finger control motor approach.

trajectory similar to that produced by the human control motor. Two approaches to producing handwriting trajectories have been identified: 1) the space oriented models which approach the trajectory formation on the basis of the capability of expressing and controlling the trajectory of the hand in space; and 2) the muscle oriented models which attempt to relate the trajectory formation to the muscle geometry and muscle properties [34]. The existing space oriented models of handwriting comply with the hypothesis that handwritten trajectories are divided into simple strokes which can be composed by concatenating them and smoothing the transition between consecutive segments. To preserve the handwritten aspect, the composite planar trajectory should be bicubic and the linking between strokes must guarantee continuity up to the second time derivative [34].

Several methods provide rules for satisfying the two conditions simultaneously, such as composite Bezier curves and regular spline functions. A previous paper [31], proposes forming the signature trajectory by linking the trajectory points with straight lines and polynomial smoothing using a Savitsky-Golay filter [35].

In this paper, we use a simpler and equally efficient smoothing of the trajectory plan using a Kaiser filter whose finite impulse response $h^t(n)$ is defined as:

$$h^t(n) = I_o\left(\pi\beta\sqrt{1-(2n/N^t-1)^2}\right)/I_o(\pi\beta), \quad 0 \le n \le N^t; \quad 0 \; otherwise \tag{2}$$

where $I_0$is a zeroth order Modified Bessel function of the first kind. N^t+1 corresponds to the length of the filter and β is the shape factor. In this work β is fixed to zero and its variation is left for future work. We guess β could be useful for simulating some effects of ageing or handwriting disorders. As the length of the filter is related to the apparent speed of the stroke, higher speed conveys greater inertia and therefore longer filters, it is called kinematic filter.

The above procedures are useful for signatures with just flourishes and produces trajectories similar to a human being, but several issues arise when generating signatures with both a text and a flourish. Writing the text requires a finer finger control motor than writing the flourish for which the major movement is made by the forearm. The wrist usually moves during the whole signing process. Thus, according to the equivalence motor theory, for generating text and flourish we need more degrees of freedom than in the case of generating just the flourish because of the greater number of muscles involved.

Thus, we use a multi-level motor scheme based on several kinematic filters of variable length that simulate the inertia of the different muscles used for handwriting. Note that this is an operational approach not necessarily related to real muscles or movements. In short, our proposal relies on three kinematic filters which are heuristically related to the finger, forearm and wrist applied as follows:

1. For the signature text, the trajectory points are linked by straight lines and divided into strokes. These are defined for each letter plan. Fig. 5.a shows an example of stroke division.

2. The finger speed profile is then estimated. The profile of each stroke j at the pixel t is obtained as $v_j^t = D_{j,1}\Lambda\left(t;\tau_{j,1},\mu_{j,1},\sigma_{j,1}^2\right) - D_{j,2}\,\Lambda\left(t;\tau_{j,2},\mu_{j,2},\sigma_{j,2}^2\right)$ following the Delta-lognormal model. The parameters $D_{j,1}, D_{j,2}, \tau_{j,1}, \tau_{j,2}, \mu_{j,1}, \mu_{j,2}, \sigma_{j,1}^2, \sigma_{j,2}^2$ are fixed for each identity since they represent the identity's motor system. The parameter values are obtained randomly in the range given by [33]. Finally, the finger speed profile v_f^t of the signature text is obtained by adding the stroke speed profiles as $v_f^t = \sum_{j=1}^{ns} v_j^t$ where ns is the number of strokes. The v_f^t is normalized to a maximum value equal to 1. It is actually a scalar version of the sigma lognormal model [35]. An example can be seen at Fig. 5.b.

3. The finger speed profile is used to select the length of the kinematic filter that programs the finger control motor. The kinematic filter length at pixel t is calculated as $N_f^t = LPsi_f \times v_f^t$ where $LPsi_f$ is a user constant which depends on the image resolution and the mean speed of the finger. The result of applying the inertia filter can be seen at Fig. 5.c. where we suppose that $LPsi_f$ is equal to the maximum distance between columns or rows of the trajectory grid.

4. For the flourish, straight lines link the flourish trajectory points. Each corner is marked as a new stroke. The Delta lognormal parameters of each stroke are randomly worked out and the flourish speed profile v_h^t is obtained by adding the speed of each stroke. In this case, the filter length is obtained as $N_h^t = LPsi_h \times v_h^t$. We use $LPsi_h$ instead of $LPsi_f$ because the motor system for the flourish is different from the motor system for the signature text. As the flourish is written quicker than the text, so $LPsi_h > LPsi_f$.

The result of applying the text and flourish kinematic filters can be seen at Fig. 6.b and Fig. 6.c respectively.

5. The wrist moves continuously when writing both the signature text and flourish. Thus we apply a third kinematic filter to the signature. In this case, the strokes are considered as the groups of connected letters (a word with all the letters connected, several connected letters, an isolated letter, etc.). The Delta lognormal parameters are

This article has been accepted for publication in a future issue of this journal, but has not been fully edited. Content may change prior to final publication. Citation information: DOI 10.1109/TPAMI.2014.2343981, IEEE Transactions on Pattern Analysis and Machine Intelligence

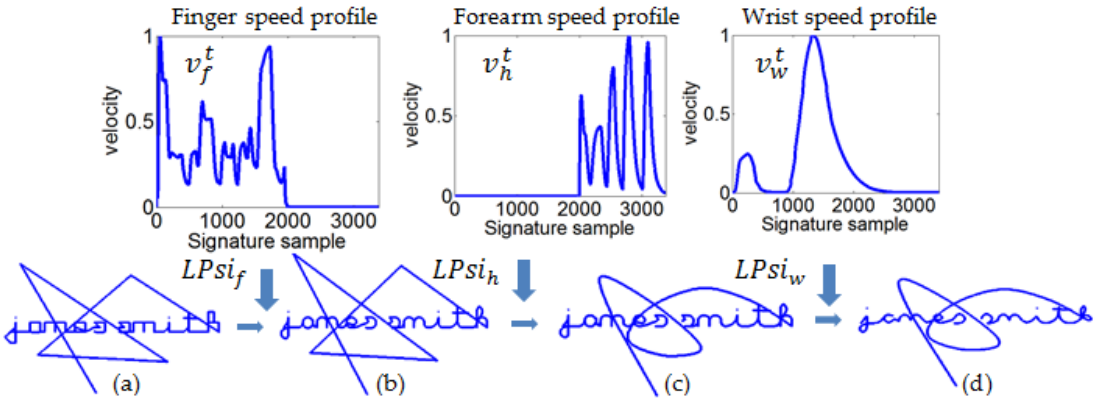

Fig. 6. a) Trajectory plan of the signature, b) result of applying the finger kinematic filter, c) result of filtering by the forearm kinematic filter and, d) signature after applying the wrist kinematic filter.

obtained for each stroke randomly and the wrist speed profile v_w^t is calculated. The kinematic filter length is obtained at each pixel as $N_w^t = LPsi_w \times v_w^t$. Fig. 6.d show an example of applying the wrist kinematic filter when $LPsi_w$ is two times the maximum distance between columns or rows of the trajectory grid.

4 Ink Model for Realistic Images

The tool used most for handwriting is the ballpoint pen. So we have used the ink deposition model of a ballpoint to produce realistic images, as at [31][37].

The ballpoint pen is a writing instrument which dispenses ink from an internal reservoir through the rolling action of a metal ball at its tip. Mainly due to ink viscosity and gravity or reservoir pressure, the ink flows from the reservoir to coat the ball. Handwriting is produced by rolling the ball on a sheet which deposits the ink on the paper. Our model supposes that the ballpoint pen generates a sequence of inked spots when rolling.

The spot shape is modelled as an ellipse the vertical and horizontal axes of which are given by $\phi_v = \phi_s \cos\beta$ and $\phi_u = \sqrt{2\phi_s\phi_v - \phi_v^2}$ where ϕ_s is the pen tip diameter and β the pen inclination angle. The major axis of the ellipse is perpendicular to the pen azimuth θ. Both are calculated by supposing that a pen pivot is located 2.5 cm from the lower right hand corner of the paper and at 2.5 cm above the paper. This assumes an average hand size.

Although the pen speed and pressure are not always correlated [38], this paper assumes that the spot gray level amplitude is inversely proportional to the speed. Let the pen speed at dot (x^t, y^t) be equal to $v_p^t = LPsi_f \times v_f^t + LPsi_h \times v_h^t + LPsi_w \times v_w^t$. The normalized pressure is presumed to be $p^t = 1/\left(v_p^t / \max v_p^t\right)$. The spot gray level amplitude is defined as $A^t = p^t \times \Delta p + p_{min}$ where Δp and p_{min} are random numbers in the range $[0 - 0.3]$ and $[0.6 - 0.8]$ respectively. To take into account the pen tip irregularities or deposition failures, the spot is multiplied by a random normal noisy spot defined as $N(0.75,0.25)$. The signature images is obtained by overlapping the consecutive spots so as to correspond to the rolling action of the ballpoint pen. The maximum dark value is taken into account by cropping the signature level intensity to $2\phi_s$.

The last step in improving the realism of the off-line signature images is to approximate the calculated stroke gray level histogram to a real ink histogram distribution. The histogram of the generated strokes is equalized to match one of the ink histograms of the three more usual ink types: fluid, viscose and solid [39].

These inks plus the usual commercial ball pen diameters $\phi_s = \{0.2, 0.25, 0.3, 0.35, 0.4, \ 0.45\}$ mm mean that 18 pen types are available. Additionally, the variables Δp, p_{min} are randomly generated for each signature. An example of the result can be seen in Fig. 7. The effect is realistic although there is room for improvements, e.g. to create striated ink deposition.

5 Synthetic Signature Parameters for Database Generation

A signature database contains several genuine samples of the same signer plus several forgeries of each signer made by different forgers. Each genuine signature is different from the others and the difference among them is called the within class variability. The differences between the different signers is called the between class variability. For synthetic signature generation, the between variability is obtained by changing the parameters that generate the signatures.

These parameters are divided into three groups. The first group contains the parameters needed to generate the morphology and lexicon of the signature. We understand these terms to mean respectively the form and formation, i.e., the number of words, letters per word, whether the signature has a flourish, the relationship between the text and flourish length and so on. The second and third groups include the parameters required to generate the trajectory plan and the motor control parameters respectively.

To obtain realistic synthetic signatures, most of the parameters range has been obtained by the analysis of real signatures databases as detailed in the next section.

This article has been accepted for publication in a future issue of this journal, but has not been fully edited. Content may change prior to final publication. Citation information: DOI 10.1109/TPAMI.2014.2343981, IEEE Transactions on Pattern Analysis and Machine Intelligence

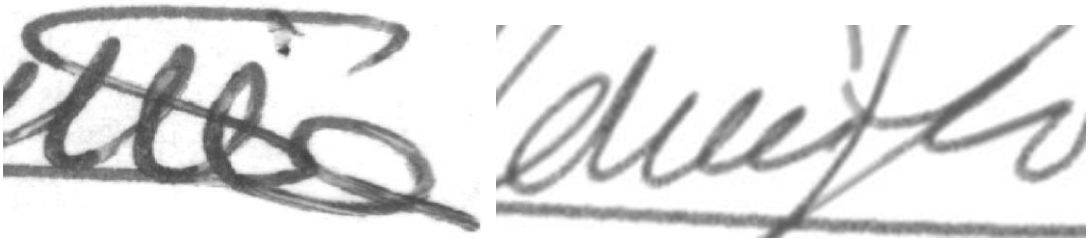

Fig. 7. Real signature stroke detail from GPDS database (left); detail of synthetic (right).

5.1 Real Database Analysis for Defining the Parameters Range of Synthetic signatures

The database analysis of real signatures has been performed by manual counting of the parameters needed for producing synthetic signatures and their frequency modeled by a probability density function (pdf) estimated by the histogram method. Two public Western off-line corpuses have been used for the counting: the MCYT and GPDS databases.

The MCYT off line database [7] includes 75 signers, 15 genuine signatures and 15 deliberate or skilled forgeries for each signer. All signature data was acquired with the same pen and the same paper templates.

The GPDS960GraySignature corpus [41] contains 24 genuine signatures and 30 deliberate forgeries from 881 individuals. The genuine signatures were written with the same ink and the forgeries with 10 different inks. Both databases were scanned at 600dpi with 256 gray levels.

The peculiarities we examined which allow the generation of a more realistic synthetic database imitating the proportions of a real database are listed below:

1. The measured probability of signatures containing flourish and text is 86.6%. The probability of signatures with only either a flourish or a text is 8.3% and 5.1% respectively.

2. Fig. 8.a shows the distribution of words in the signature, up to the third word. Those with one word: 50%, with two words: 36.3% and with three words: 13.7%.

3. Fig. 8.b shows the distribution of the number of letters per signature. This is modeled by a normal distribution of mean 5.5 and sigma 2.2.

4. The number of flourish corners is related to the flourish complexity which is a relevant signature parameter. Fig. 8.c shows the distribution of the number of flourish corners which is approximate by a lognormal distribution of $\mu = 1.59$ and $\sigma = 0.42$ which corresponds to a mean equal 5.38 and variance equal to 5.5. As real signatures can include two flourishes, the second one is approximated by using the same probability distribution with $\mu = 1.37$ and $\sigma = 0.28$.

5. Some signatures have wider texts in relation to the flourish widths than others. To model this fact, the distribution of the ratio between the text and flourish widths is worked out and represented in Fig. 8.d. This distribution can be fitted by a lognormal distribution of $\mu = -0.22$ and $\sigma = 0.38$ which corresponds to a mean equal to 0.85 and variance equal to 0.11.

6. Real signatures present an inclination or skew. This is measured by enveloping the signature by an ellipse and working out the angle of the major axis. Fig. 8.e shows the distribution of the measured skew which is approximated by a generalized extreme value probability density function with shape parameter $\xi = -0.12$, scale parameter $\sigma = 7.68$ and a location parameter $\mu = 2.43$.

7. Similarly, the slant effect is another personal feature needed to imitate the generation of synthetic signatures. The estimated distribution of the signature slant is depicted at Fig. 8.f. It suggests again a generalized extreme value probability density function but with a shape $\xi = -0.16$, scale $\sigma = 11.54$, and a location $\mu = -0.21$.

8. The distribution of the letter size, in terms of their width in millimeters, in the above mentioned databases is shown at Fig. 8.g. It can be approximated by a normal distribution of $\mu = 3.00$ and $\sigma = 0.62$.

9. The distribution of the space in millimeters between letters is shown at Fig. 8.h. It can be approximated by a normal distribution of $\mu = 1.17$ and $\sigma = 0.20$.

10. Fig. 8.i estimates the distribution of the space between words in millimeters as a normal distribution of $\mu = 8.00$ and $\sigma = 0.89$.

Other interesting data we use to help generate the synthetic database are as follows:

- The probability of connecting the last letter of the text with the beginning of the flourish is fixed at 58%.
- Of the signatures with a flourish, 81% have just one flourish and 19% of them have a second non-connected flourish.
- The probability of all the letters being connected is 59%.

5.2 Parameters to Generate a Synthetic Signature

The parameters we use to generate automatically the signature of a new synthetic identity are given in three groups below.

<u>Parameters to define the signature lexical morphology</u>

1. $Ptext, Pflourish, Ptext\&flourish$: Probability that the signature includes only text, only flourish or text plus flourish. Their values are obtained from the real database counting given at section 5.1.

2. $Pconnect$: Probability of the text and the flourish being connected. This is worked out with the probability given at section 5.1.

3. $Nwords$: Number of words in the signature text, obtained with the pdf of Fig. 8.a.

4. $Nletters$: Number of letters in each word, as in pdf from Fig. 8.b.

5. $Name$: Signature text, for instance "James Smith". The text is randomly obtained taking into account the occur-

This article has been accepted for publication in a future issue of this journal, but has not been fully edited. Content may change prior to final publication. Citation information: DOI 10.1109/TPAMI.2014.2343981, IEEE Transactions on Pattern Analysis and Machine Intelligence

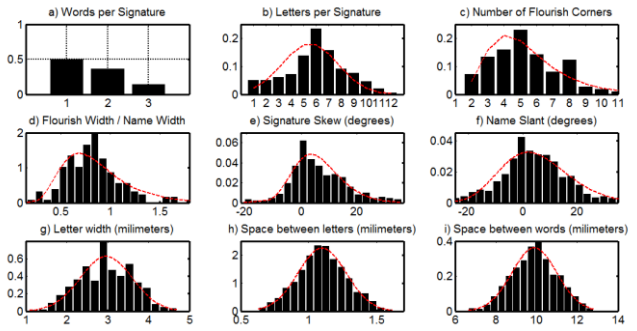

Fig. 8. Distribution of modeled features from real off-line signatures from MCYT and GPDS database and their approximated pdfs.

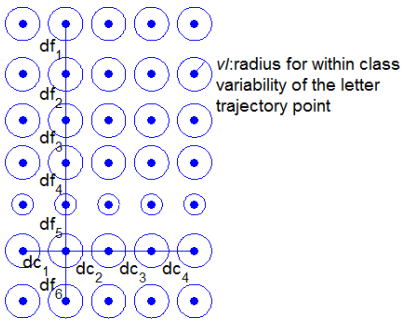

Fig. 9. Definition of the distance between columns dc_i and rows df_i of the grid trajectory points and the radius vl and vbl for within word letter class variability.

rence probability of each letter in the English language. So, we do not automatically generate real texts but fictitious texts as corresponds to synthetic signatures.

6. Pul: Probability of all the letters of the text being joined, as modeled at section 5.1

7. Nf: Number of flourishes, as modeled at section 5.1.

8. Nc: The number of corners per flourish obtained from the distribution in Fig. 8.c. The positions of the corners $c_i = (xrc_i, yrc_i)_{i=1}^{Nc}$ are located as defined at section 2.2.

Parameters to generate the trajectory plan

9. $c_i = (xrc_i, yrc_i)_{i=1}^{Nc}$: Positions of the flourish corners obtained as defined at section 2.2.

10. $\{dc_i\}_{i=1}^{4}$: The distance between columns of the grid trajectory points (see Fig. 9) that define the letter shape and size. Taking into account the distribution at Fig. 8.g and a 600dpi image, this is obtained randomly in the range [5−30] pixels for each identity.

11. $\{df_i\}_{i=1}^{6}$: Distance between rows of the grid trajectory points defined in the same way as dc_i.

12. swr: This defines the ratio $(Text\ Width/\ Flourish\ Width)$ which is obtained randomly from the distribution of Fig. 8.d. The ratio is fitted to the synthetic signature by estimating:

$$l2f = \left(\max_i(xrc_i) - \min_i(xrc_i)\right) / \left(\Sigma(Nletters) \times \sum_i(dc_i)\right) \quad (5)$$

and scaling the letter size as follows: $dc_i = dc_i \times l2f \times swr$ and $df_i = df_i \times l2f \times swr$.

13. vl: Variability of the letter. A letter is never written in exactly the same way by a writer, so we introduce a variable to control the letter shape variability. This can be described as inner word variability. Each time a letter is generated, the grid trajectory points are moved inside a circle of radius is equal to vl as shown at Fig. 9. Each writer has his own variability. The radius depends on the letter size and it is heuristically fixed for each identity in the range $[0.5 \times mgrid - 1.2 \times mgrid]$ where $mgrid = min\left\{\min_i\{dc_i\}, \min_i\{df_i\}\right\}$.

14. vbl: Variability of the baseline. This is different from the variability of the other trajectory points because of the expected ability of a healthy writer to write on or close to a straight line. Therefore, the variability or circle radius of the trajectory points 5, 12, 19, 26 and 33 is smaller than vl (see Fig. 9). This variable is randomly set up in the range $[0.2 \times mgrid - 1.7 \times mgrid]$ pixels for each identity.

15. sbl: Space between consecutive letters for an identity. See distribution Fig. 8.h.

16. sbw: Space between consecutive words for an identity, as modeled by Fig. 8.i.

17. $vsbl$: Variability of the space between letters. This is not constant even within the same word. So it changes among the letters and can be seen as an example of inner word variability. Therefore, each time a letter is added, the space to the prior letter is obtained as $sbl + vsbl$ which is calculated as random value in the range $[-0.7 \times mgrid - 0.7 \times mgrid]$ pixels. This range has been heuristically adjusted.

18. $vsbw$: Variability of the space between words. As in the case of $vsbl$, each time a word is added, the space to the prior word is obtained as $sbw + vsbw$ which is calculated as a random variable in the heuristic range $[-4 \times mgrid - 4 \times mgrid]$ pixels.

19. $skew$: The signature skew is modeled as Fig. 8.e and is accomplished by rotating the signature trajectory plan.

20. $slant$: The slant of the handwriting. Following the distribution of Fig. 8.f, this is achieved by applying an affine transformation to the text trajectory plan.

Parameters to generate the motor control approach

The values of the following four parameters are inspired by [33]. The last four have been set heuristically:

21. $Medialogn$: Location parameter μ of the agonist log normal distribution. This is used to obtain the velocity profile. Randomly defined in the range [-0.7−0].

22. $Varalogn$: scale parameter σ of the agonist log normal distribution. This is used to obtain the velocity profile. Randomly assigned to the identity in the range [0.2−0.6].

23. $Medialogna$: Location parameter of the antagonist lognormal distribution. This is used to obtain the velocity profile. Randomly worked out in the range [-0.5−0.7].

24. $Varlogna$: Scale parameter of the antagonist lognormal distribution. This is used to obtain the velocity profile. In the range [0.2−0.6].

25. $LPsi_f$: Length of the smoothing filter for the finger motor model. This variable depends on the letter size, so its range is defined between $[1.5 \times mgrid - 4 \times mgrid]$.

26. $LPsi_h$: Length of the smoothing filter for the forearm motor model. This variable depends on the flourish size.

This article has been accepted for publication in a future issue of this journal, but has not been fully edited. Content may change prior to final publication. Citation information: DOI 10.1109/TPAMI.2014.2343981, IEEE Transactions on Pattern Analysis and Machine Intelligence

Fig. 10. Influence of increasing the kinetic filters length$LPsi_f$, $LPsi_h$ and $LPsi_w$ on the signature readability

This is Ml times the maximum of the distances between the flourish corners. The range of this variable is $[0.6 \times Ml - 1.2 \times Ml]$.

27. $LPsi_w$: Length of the smoothing filter for the wrist motor model. From experiments we conducted, the range of this variable is set between $[1.0 \times mgrid - 3 \times mgrid]$.

By varying these parameters randomly, according to their probability density function, 98% of the cases found in the real databases can be generated by the synthesizer. One example of a signature that the synthesizer cannot generate one with two lines of text.

It is possible to generate signatures with just a text line ($Ptext = 1$ and $Pflourish = 0$) or only a flourish ($Ptext = 0$ and $Pflourish = 1$). For signature with text and a flourish both parameters are equal to 1.

The complexity of the text line is set up by parameters $Nwords$ and $Nletters$ which correspond to the number of words and letters in the signature text. The signature complexity increases with the number of words and letters.

On the other hand, the complexity of the flourish is adjusted by the parameter Nf and Nc which corresponds to the number of flourishes and number of corners in the flourish. If the number of flourishes or corners increases, the signature is more complex.

The readability of the signature is related to the length the kinetic filters whose parameters are called $LPsi_f$, $LPsi_h$ and $LPsi_w$. If the value of these parameters increases, this implies an increase in the handwriting speed, resulting in the text line becoming less and less legible.

Fig. 10 show the change in text line readability as the kinematic filter length is increased.

5.3 Parameters to Generate Multiple Samples of a Synthetic Identity

The above variables allow us to generate the master signature of a new synthetic identity. In this section we describe the procedure required to define the synthetic signer stability or the within variability, i.e. the differences between multiple genuine samples.

In this paper, the within variability is controlled by two parameters. The first refers to the flourish and the second to the text and neuromuscular kinematic filters. These parameters are:

1. $rballg$: Radius of flourish corner ball. We introduce the variability in the flourish by changing the position of the corners of the flourish. The new corners lie inside a ball of radius $rballg$ around the user corners $(xrc_i, yrc_i)_{i=1}^{Nc}$.

2. wnv: Within text variability. Each time a signer produces a new signature, it keeps the same cognitive map and action plan but the neuromuscular path slightly changes its conditions due to different posture, equilibrium condition, etc. therefore introducing slight differences in the handwritten text. In the synthetized signature this is modeled by changing the value of the following text parameters: vl, vbl, sbl, sbw, $vsbl$, $vsbw$, $slant$, $skew$, $LPsi_f$, $LPsi_h$ and $LPsi_w$. With the variable wnv we define the percentage that each variable changes, i.e., for the new synthetic signature sample the new vl value will be a random number between $[vl - vl \times wnv/100 - vl + vl \times wnv/100]$ and so on. Obviously, we check that the newly obtained values are within the given parameter range. Otherwise, the maximum or minimum value is assigned, depending on which values exceed the range.

The within variability of the identity will be proportional to $rballg$ and wnv.

5.4 Parameters to Generate Forgery Samples

In the case of forgery generation, as the forger imitates the genuine signature, he or she will try to extract the action plan from the original signature, so the forger follows a similar trajectory to the genuine signature but with a higher variability than the within class variability because of mistakes in the reconstruction of the action plan and the different neuromuscular systems between the forger and genuine signer.

The above principles are summarized in two parameters, the first related to the flourish and the second to the text. These variables are:

1. $rballf$: Radius of the forgery flourish ring. As in the case of genuine identity, the flourishes made by a synthetic forger are generated by moving the flourish corners. To simulate the greater variability of the forgers and their difficulties in capturing the exact corner position, we use a ring instead of a ball. Therefore $rballf$ is a vector comprising the inner and an outer ring radius. The bigger the intersection area between the genuine ball and the forgery ring, the more skilled the forger.

2. fnv: Forger text variability. This parameter is intended to simulate the forger variability for writing the text. As in the case of wnv, it expresses the percentage variability in respect the parameter value but in this case it consists of two values: $fnv(1)$ and $fnv(2)$. The first indicates the minimum variability and the second the maximum variability. For example, the vl value for a forger is a random value in the range:

$$\left[vl - vl\frac{fnv(2)}{100}, vl - vl\frac{fnv(1)}{100}\right] \cup \left[vl + vl\frac{fnv(1)}{100}, vl + vl\frac{fnv(2)}{100}\right]$$

If the modified value is not in the parameter range, it is set to its nearest extreme value. The modified parameters are:

a. As in the case of genuine generation: vl, vbl, sbl, sbw, $vsbl$, $vsbw$, $slant$, $skew$, $LPsi_f$, $LPsi_h$ and $LPsi_w$.

b. Additionally, as the forger does not capture the exact

This article has been accepted for publication in a future issue of this journal, but has not been fully edited. Content may change prior to final publication. Citation information: DOI 10.1109/TPAMI.2014.2343981, IEEE Transactions on Pattern Analysis and Machine Intelligence

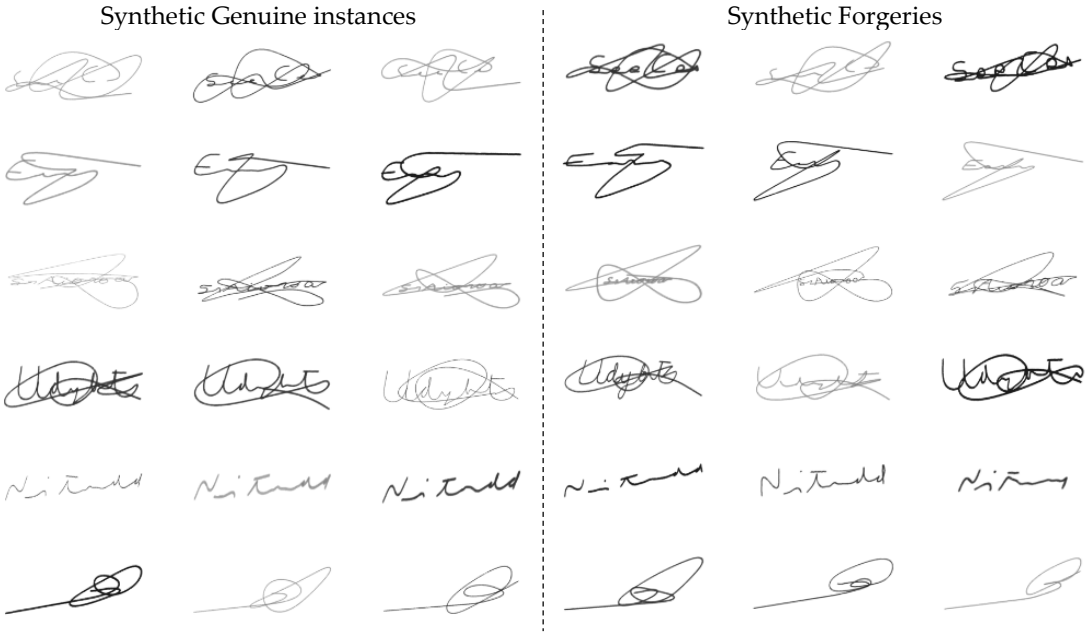

Fig. 11. Six possible synthetic identities with three genuine specimens (first three columns) and three possible forged signatures (last three columns). The first four signatures are composed of text plus flourish, the fifth example has only text and the sixth is a simple flourish.

letter grid from the genuine signature, the letter grid values $\{dc_i\}_{i=1}^{4}$ and $\{df_i\}_{i=1}^{6}$ are also modified by fnv.

c. Finally, as a forger has a different neuromuscular system, the values of variables $Medialogn$, $Varlogn$, $Medialogna$ and $Varlogna$ are worked out anew but as the forger forces his own neuromuscular system to imitate the genuine signature shape the variables $LPsi_f$, $LPsi_h$ and $LPsi_w$ are modified by fnv as said above.

Fig. 11 shows different examples of synthetic genuine and forged signatures obtained by the procedures described: it displays signature with both flourish and text with different complexities, a signature with only text and another one with just a flourish.

6 Experiments

These experiments are aimed at determining the ability of the synthesizer to generate realistic synthetic datasets. The stability of the genuine signatures and the skills of the synthetic forgers are customized by adjusting the values of the variables: $rballg$, $rballf$, wnv and fnv.

Therefore, two kinds of experiments have been carried out: perceptual experiments to assess the realism of the synthetic signature images and performance experiments on generated synthetic databases to validate in terms of Equal Error Rate (EER) the synthetic signer variability and the forgers' skills.

The performance experiments are carried out in two steps. The first works out the relation between the EER with random forgeries and the parameters $rballg$ and wnv which controls the within and between variability of the synthetic signature database. The second step studies the sensitivity of the EER for forgers' skill with respect to the parameters $rballf$ and fnv.

The perceptual experiment is carried out by estimating human ability to distinguish between synthetic and real signatures through a survey with people outside of the forensic area.

6.1 Protocol for Performance Experiments

The performance evaluation is computed by using the verifier proposed in [41]. It is based on texture features such as the local binary pattern (LBP) [34] and the local derivative pattern (LDP) [35]. The signature is transformed to the LBP and LDP image which is divided into 12 sectors. The histogram of each sector is worked out, concatenated and its dimension reduced by using a Discrete Cosine Transform (DCT) to obtain the feature vector. The classifier is based on a least square support vector machine (LSSVM) [36].

Following a well-established experimental protocol, the training set consists of 10 randomly selected genuine signatures. The remaining genuine signatures are used for testing. When testing with a specific signer, random forgery scores are computed by using the genuine test samples from all the remaining users. Scores for forgers are computed from the synthetic forgeries of the signer. All the experiments are repeated 10 times and the averaged results in term of Equal Error Rate (EER) are provided.

In order to establish a reference for the realism of the performance results obtained with the synthetic databases, the performance obtained with the real signatures of the GPDS corpus with 150 users are an EER=0.44% for random forgeries and EER=15.90% for skilled forgeries. For the 881 real users from the same database, the EERs are equal to 0.88% and 23.42% for random and skilled forgeries respectively.

This article has been accepted for publication in a future issue of this journal, but has not been fully edited. Content may change prior to final publication. Citation information: DOI 10.1109/TPAMI.2014.2343981, IEEE Transactions on Pattern Analysis and Machine Intelligence

6.2 Performance Experiments

This section studies the performance sensitivity with respect to the four parameters that define the database variability. First we report at Table I the sensitivity with respect to the parameters that set up the synthesis of genuine samples: $rballg$ and wnv. The ability of these parameters to produce datasets with different inner and between class variability is clear from the range of different EERs obtained. It can be seen that reducing the flourish corner ball radius, decreases the synthetic signer variability and improves the performance. Also the performance is more sensitive to $rballg$ than to wnv. Moreover, the ability of the procedure to produce realistic databases is proved by the fact that the synthetic database performance is similar to the real GPDS database performance when $rballg = 2.96$ mm and wnv=30%.

Table II evaluates the ability of the synthetic procedure to produce forgeries with different skills. This depends on the following parameters: the inner and outer radius of the flourish corner ring for forgeries $rballf(1)$ and $rballf(2)$ and the forger text variability fnv. Table II presents the results for various $rballf(2)$ and fnv, supposing for the sake of simplicity that $rballf(1) = 3.77$ mm. The EER reduces when the outer ring radius increases because a greater $rballf(2)$ means less skilled forgers. Again, $rballf$ influences the performance more than fnv because it is the former variable which best describes the forgers' skills. Similar results to those for a real GPDS database can be obtained by setting $rballf(2) = 6.70$ mm and wnv=100%.

In conclusion, the proposed procedure is able to generate useful customized databases. The different variabilities and therefore performances are tuned according to only four parameters.

TABLE I
EER (%) FOR RANDOM FORGERIES FOR 150 SYNTHETIC USERS

Within text variability: wnv	Ring corner ball radius: $rballg$ in mm					
	0.42	1.27	2.12	2.96	3.81	4.66
10 %	0.0000	0.023	0.09	0.33	0.61	1.60
30 %	0.0003	0.010	0.10	0.45	0.79	1.61
50 %	0.0006	0.01	0.11	0.48	0.85	1.74
70%	0.002	0.09	0.19	0.56	1.30	2.17
90%	0.006	0.09	0.28	0.64	1.85	2.38

TABLE II
EER (%) FOR SKILLED FORGERIES WITH 150 SYNTHETIC USERS*

Forger text variability: fnv	Outer ring corner ball radius $rballf(2)$ in mm				
	5.77	6.28	6.70	7.13	7.55
60 %	18.16	16.86	15.72	15.17	14.56
80 %	16.98	16.17	15.36	14.80	13.66
100 %	16.61	16.09	15.56	14.30	12.53
120 %	15.57	15.24	14.91	13.23	11.91
140 %	14.30	14.38	14.45	12.55	12.97

*The inner ring corner ball is fixed to $rballf(1) = 3.77$ mm

6.3 Perceptual experiments

We conduct perceptual experiments to investigate the generator's ability to produce humanlike signatures. In a similar way to [20] [37][45], this is measured by showing non-forensic volunteers a set of real and synthetic images. The volunteers are not told whether the signature is real or synthetic. They are asked to score between 0 (very sure synthetic) and 10 (very sure human) the realism of the presented signature according to their impression, formed after a quick inspection of the signature.

Fig. 12. Subset of signatures used in the Perceptual Experiment to evaluate the appearance of our signatures. For information, the synthetic signatures are marked with a cross.

For this experiment, forty synthetic signatures were generated with real texts. They were combined with another 40 real signatures randomly selected from GPDS, MCYT. Real and synthetic signatures were randomly mixed.

To avoid any background effects, the signatures were set against the same white background. In addition, the test was presented on printed sheets to avoid the use of computer facilities, e.g. the zoom, to help make the decision. A subset of this experiment is shown in Fig. 12

The realism of the synthetic generator is measured by calculating two kinds of errors, as in [20] and [37]. We work out the False Synthetic Rate (FSR): a real signature is assigned as synthetic if the score is less than 5. We then work out the False Real Rate (FRR): a synthetic signature is assigned as real if its score is greater than 5. The final Average Classification Error (ACE) is calculated as ACE= (FSR + FRR)/2. The results of the survey of 80 volunteers are shown in the first three columns of Table III. The average score of real and synthetic signatures is also given at Table III along with the average time taken to complete the experiment.

TABLE III
RESULTS OF THE PERCEPTUAL EXPERIMENT

Error rates (%)			Average score		Average time (min)
FSR	FRR	ACE	Real	Synthetic	
43.02	45.10	44.06	5.38	4.50	8.70

This article has been accepted for publication in a future issue of this journal, but has not been fully edited. Content may change prior to final publication. Citation information: DOI 10.1109/TPAMI.2014.2343981, IEEE Transactions on Pattern Analysis and Machine Intelligence

The value of ACE=44.06% confirms the expected confusion between real and synthetic signatures. This conclusion is also supported by the real and synthetic average score of around 5. Therefore, we conclude that perceptually the synthetic signature generator based on the motor equivalence approach along with the virtual deposition ink model is able to produce signatures that human non-expert examiners accept as real.

7 Case Study: Robustness against number of identities and ink variability

An advantage of our synthetic signature generator is that it allows easy checking of the robustness of verification algorithms according to different scenarios. In this section, as a useful example of applying the synthetic algorithm, we analyze the robustness of the signature verifier to different numbers of users and inks. Five versions of the same database are generated for the following 5 experiments:

- *Experiment 1:* Generation of a database by assigning a random pen to each sample. Our pen model considers 18 possible types of pen. The pen diameter varies in the range {0.2 0.25 0.3 0.35 0.4 0.45} *mm* and the ink type is randomly chosen from solid, viscous and fluid.
- *Experiment 2:* Signature images for all the samples are generated with a ballpoint of 0.4 mm and solid ink. This is similar to the pen used for the off-line MCYT signature database.
- *Experiment 3:* In this case, the images are generated with a ballpoint of diameter 0.2 mm and viscous ink.
- *Experiment 4:* The images are obtained with a ballpoint of diameter 0.2 mm and solid ink.
- *Experiment 5:* As in the case of GPDS, the genuine signature of each synthetic identity is generated using the same randomly selected pen. The forgeries are synthesized with a randomly selected pen.

By comparing the results of experiments 2 and 4 we can see the influence of the ballpoint diameter on the signature verifier. Also, we can see the effect of varying the ink type by comparing the results from experiments 3 and 4. The influence of the pen can be seen in experiment 5 where the random and simulated forgeries have been written with a different pen than that used for the genuine signatures. Experiment 1 shows the most realistic case because each sample is written with a different pen.

TABLE IV
EER FOR RANDOM FORGERIES OF THE SAME SYNTHETIC DB WITH DIFFERENT PEN CONFIGURATIONS AND NUMBER OF USERS

			Number of users in the database						
Exp	ballpoint	ink	75	150	300	881	1500	2500	4000
1	random	random	0.76	0.57	0.63	0.79	0.79	0.74	0.79
2	4 mm	solid	0.53	0.52	0.44	0.72	0.72	0.63	0.67
3	2 mm	viscous	0.48	0.51	0.45	0.75	0.70	0.67	0.71
4	2 mm	solid	0.47	0.55	0.54	0.73	0.71	0.64	0.68
5	Random (same for all the genuine)		0.47	0.47	0.47	0.66	0.62	0.57	0.61

Table IV shows the results of the above experiments using a different number of identities. Increasing the number of identities does not display a clear tendency in the EER. This indicates that the EER depends more on the identities' variability than on their number. On the other hand, randomly changing the ink decreases the performance. From comparing experiment 2 and 4, it seems that narrower ballpoints make verification easier; and by comparing the third and fourth experiments, it appears that the ink type is not relevant in a database when all the signatures are taken with the same ink type. The comparison of the first experiment (randomly selected inks) with the second (all users with the same ink as in the MCYT database) and fifth (each user with one ink type as in GPDS database) indicates that the results obtained with the GPDS and MCYT databases are biased positively with respect to real applications where each signer uses a different pen for each signature.

8 Conclusion

This paper proposes a novel method for the generation of synthetic off-line handwritten signatures inspired by the human neuromotor model. The proposed method generates entirely realistic synthetic genuine and synthetic forged signatures. Additionally, an ink deposition model is used to generate images with a highly realistic appearance.

The designed synthetic signature generator is based on the so called internal model which defines the handwriting action in two steps: the action plan and neuromotor inverse model. The signature generator imitates the action plan by using a trajectory plan, i.e. a sequence of target trajectory points in a grid. The neuromotor path is represented by a kinematic filter based on a variable length Kaiser window. The window length is proportional to the inverse of the pen speed, which is obtained using a scalar version of the sigma lognormal model. Once the synthetic signature's trajectory is worked out, an ink deposition model is defined to obtain realistic images of the signature generated.

The parameters we use to define the synthesized signature are obtained by analyzing the lexical and morphological aspects of signatures in the MCYT Off-line signature and GPDS signature corpus. Parameters such as the number of words in a real signature, the number of letters per word, the presence or absence of a flourish or text, text and flourish relations, etc. have been statistically characterized.

The validation protocol is twofold: performance related and perceptual. The performance experiment is aimed at learning the ability of the synthetic signature generator to produce databases with different within class variability and forgeries with different forger skills. The experiments show that by varying only four variables it is possible to control the writer stability and the forger skill. It is possible to find values of these parameters to synthetize databases with a similar performance to a real database such as the GPDS.

The perceptual experiment is addressed at learning the ability of the synthesizer to generate humanlike signatures. A survey to 80 people shows a near 50% of confusion between real and synthetic signatures which proves the realism of the generated synthetic signatures.

The novel synthetic generation algorithm has enormous potential for many applications such as performance estimation, security evaluation, scalability studies, ink effect studies, etc. Some of them are evaluated in this paper. In our on-going research we are adding parameters to test temporal drift to the database to simulate the effects of multisession signature taking, ageing and neurodegenerative illness. We believe forgery generation can be also improved by using the ScriptStudio program [46].

ACKNOWLEDGMENTS

This study was funded by the Spanish government's MCINN TEC2012-38630-C04-02 research project.

REFERENCES

[1] A. K. Jain, A. A. Ross, K. Nandakumar, *Introduction to Biometrics*, Springer, 2011

[2] S. Z. Li, A. K. Jain (Eds.), *Handbook of Face Recognition*, Springer, 2nd edition, 2011.

[3] D. Maltoni, D. Maio, A. Jain, S. Prabhakar, *Handbook of Fingerprint Recognition*, Springer, 2009.

[4] J. Daugman, "How iris recognition works", *IEEE Transactions on Circuits and Systems for Video Technology* , vol. 14, pp. 21–30, Jan. 2004.

[5] ISO/IEC 19795-X, Biometric Testing & Reporting, defined by SC67 WG4.

[6] A. J. Mansfield and J. L. Waymen, Best Practices in Testing and Reporting Performance of Biometric Devices, Version 2.0, NPL Report CMSC 14/02, National Physical Laboratory, San Jose State University, Aug. 2002.

[7] J. Fierrez-Aguilar, N. Alonso-Hermira, G. Moreno-Marquez, and J. Ortega-Garcia, "An off-line signature verification system based on fusion of local and global information", *Workshop on Biometric Authentication*, Springer LNCS-3087, pp. 298–306, May 2004.

[8] GAVAB offline signature database, available at: http://www.gavab.es/recursos.html#firmas

[9] Biosecure Signature Database. Available at: http://biometrics.it-sudparis.eu/ESRA2011/

[10] J. Ortega-Garcia, J. Fierrez, F. Alonso-Fernandez, J. Galbally, M.R. Freire, J. Gonzalez-Rodriguez, C. Garcia-Mateo, J.L. Alba-Castro, E. Gonzalez-Agulla, E. Otero-Muras, S. Garcia-Salicetti, L. Allano, B. Ly-Van, B. Dorizzi, J. Kittler, T. Bourlai, N. Poh, F. Deravi, M. Ng, M. Fairhurst, J. Hennebert, A. Humm, M. Tistarelli, L. Brodo, J. Richiardi, A. Drygajlo, H. Ganster, F.M. Sukno, S.K.Pavani, A. Frangi, L. Akarun, A. Savran, "The Multiscenario Multienvironment BioSecure Multimodal Database (BMDB)", *IEEE Transactions on Pattern Analysis and Machine Intelligence,* vol. 32, no. 6, pp. 1097-1111, Jun. 2010.

[11] R. Cappelli, "Synthetic Fingerprint Generation", in D. Maltoni, D.Maio, A. K. Jain, and S. Prabhakar, Eds., *Handbook of Fingerprint Recognition*, Springer, pp. 203-232, 2003.

[12] M. Rejman-Greene, *Privacy issues in the application of biometrics: a European perspective*, Biometric Systems. Technology, design and performance evaluation, Springer, pp. 335–359, 2005

[13] N. Poh, S. Marcel, S. Bengio, "Improving face authentication using virtual samples", *Proc. of the IEEE Int. Conf. on Acoustics, Speech and Signal Processing (ICASSP)*, pp. 233-236, Apr. 2003.

[14] J. Zuo, N. A. Schmid, X. Chen, "On generation and analysis of synthetic iris images", *IEEE Trans. on Information Forensics and Security*, vol. 2, pp. 77-90, Mar. 2007.

[15] T. Dutoit, *An Introduction to Text-to-Speech Synthesis*, Kluwer Academic Publishers, 2001.

[16] A. Lin, L. Wang, "Style preserving English handwriting synthesis", *Pattern Recognition*, vol, 40, pp. 2097-2109, Jul. 2007.

[17] D. V. Popel, "Signature analysis, verification and synthesis in pervasive environments", *Synthesis and Analysis in Biometrics*, World Scientific, pp. 31–63, May 2007.

[18] C. Rabasse, M. Guest, C. Fairhurst, "A New Method for the Synthesis of Signature Data With Natural Variability", *IEEE Trans. on System, Man, and Cybernetics – Part B*, vol. 38, no. 3, Jun. 2008

[19] J. Galbally, R. Plamondon, J. Fierrez and J. Ortega-Garcia, "Synthetic on-line signature generation. Part I: Methodology and algorithms", *Pattern Recognition*, vol. 45, pp. 2610-2621, Jul. 2012.

[20] J. Galbally, J. Fierrez, J. Ortega-García, R. Plamondon, "Synthetic on-line signature generation. Part II: Experimental validation", *Pattern Recognition*, vol. 45, pp. 2622-2632, Jul. 2012.

[21] J. Galbally, J. Fierrez, M. Martinez-Diaz, J. Ortega-Garcia, "Improving the enrollment in dynamic signature verification with synthetic samples", *Proc. of the IAPR Int. Conf. on Document Analysis and Recognition* (ICDAR), pp. 1295-1299, Jul. 2009.

[22] Karl S. Lashley, "Basic Neural Mechanism in Behavior", *Psychological Review*, vol. 37, pp. 1-24, 1930.

[23] Nikolai A. Bernstein, *The Co-ordination and Regulation of Movements*, Oxford: Pergamon Press, 1967.

[24] Angeo Marcelli, Antonio Parziale, Rosa Senatore, "Some Observations on Handwriting from a Motor Learning Perspective", *2nd Workshop on Automated Forensic Handwriting Analysis,* Washington DC, USA, pp. 6-10, Aug. 2013.

[25] A. M. Wing, "Motor control: mechanisms of motor equivalence in handwriting", *Current Biology*, vol. 10, pp. 245–248, Mar. 2000.

[26] M. Kawato, "Internal models for motor control and trajectory planning", *Current Opinion in Neurobiology*, vol. 9, pp. 718–727, Dec. 1999.

[27] R. Plamondon, "A Kinematic Theory of Rapid Human Movements. Part I: Movement representation and generation", Biological Cybernetics, vol. 72, no. 4, pp 295-307, Mar. 1995.

[28] R. Plamondon, "A Kinematic Theory of Rapid Human Movements. Part II: Movement time and control", Biological Cybernetics, vol. 72, no. 4, pp 309-320, March 1995.

[29] R. Plamondon, "A Kinematic Theory of Rapid Human Movements. Part III: Kinematic Outcomes", Biological Cybernetics, vol. 78, no. 2, pp 133-145, Feb. 1998.

[30] R. Plamondon, "A Kinematic Theory of Rapid Human Movements. Part IV: A Formal Mathematical Proof and New Insights", Biological Cybernetics, vol. 89, no. 2, pp 126-138, Aug. 2003.

[31] Miguel A. Ferrer, Moisés Díaz-Cabrera, Aythami Morales , "Synthetic Off-line Signature Image Generation", *Proc. of 6th IAPR Int. Conf. on Biometrics*, Madrid, Spain, pp. 1-7, Jun. 2013.

[32] T. F. Cootes, C. J. Taylor, D. H. Cooper and J. Graham, "Active Shape Models – Their Training and Application", *Computer Vision and Image Understanding*, vol. 61, no. 1, pp. 38-59, Jan. 1995.

[33] M. Djioua, R. Plamondon, "A New Algorithm and System for the Characterization of Handwriting Strokes with Delta-Lognormal Parameters," *IEEE Trans. on Pattern Analysis and Machine Intelligence*, vol.31, no.11, pp.2060-2072, Nov. 2009.

[34] P. Morasso, F. A. Mussa, "Trajectory Formulation and Handwriting: A

Computational Model", *Biological Cybernetics*, vol. 45, pp. 131-142, 1982.

[35] Ronald W. Shafer, "What Is a Savitzky-Golay Filter", *IEEE Signal Processing Magazine*, pp. 111-117, Jul. 2011.

[36] Christian O'Reilly, Réjean Plamondon, "Development of a Sigma–Lognormal representation for on-line signatures", *Pattern Recognition*, Volume 42, Issue 12, pp. 3324-3337, Dec. 2009.

[37] Miguel A. Ferrer, Moises Diaz-Cabrera, Aythami Morales, Javier Galbally, Marta Gomez-Barrero. "Realistic Synthetic Off-line signature Generation Based on Synthetic On-line Data", *Proc. IEEE Int. Carnahan Conf. on Security Technology*, ICCST, Medellin, Colombia, pp. 116-121, Oct. 2013.

[38] L. R.B. Schomaker, R. Plamondon, "The Relation between Pen Force and Pen Point Kinematics in Handwriting", Biological Cybernetics, vol. 63, no. 4, pp. 277-289, Aug. 1990.

[39] K. Franke and S. Rose, "Ink-deposition model: the relation of writing and ink deposition Processes", *Proc. Ninth International Workshop on Frontiers in Handwriting Recognition*, Tokio, Japan, pp. 173 - 178, Oct. 2004.

[40] D. Coltuc, P. Bolon, and J.-M. Chassery, "Exact histogram specification", *IEEE Trans. on Image Processing*, vol. 15(5), pp. 1143 - 1152, May 2006.

[41] Miguel A. Ferrer, Francisco Vargas, Aythami Morales, Aaron Ordoñez, "Robustness of Off-line Signature Verification based on Gray Level Features", *IEEE Trans. on Information Forensics and Security*, vol. 7, no. 3, pp. 966-977, Jun. 2012.

[42] T. Ojala, M. Pietikainen, T. Maenpaa, "Multiresolution gray-scale and rotation invariant texture classification with local binary patterns", *IEEE Trans. on Pattern Analysis and Machine Intelligence*, vol. 24, no.7, pp. 971–987, 2002.

[43] T. Jabid, M. H. Kabir, O. Chae, "Local Directional Pattern (LDP) – A Robust Image Descriptor for Object Recognition", *Proc. Seventh IEEE Int. Conf. on Advanced Video and Signal Based Surveillance*, pp. 482-487, Boston, USA, Aug. 2010.

[44] J. A. K. Suykens, T. V. Gestel, J. D. Brabanter, B. D. Moor, J. Vandewalle, *Least Squares Support Vector Machines*, World Scientific Publishing Co., Pte, Ltd, Singapore, 2002.

[45] R. Cappelli, D. Maio, D. Maltoni, "Synthetic fingerprint-database generation", *Proc. 16th Int. Conf. on Pattern Recognition*, vol. 3, pp. 744-747, Aug. 2002.

[46] M. Djioua, R. Plamondon, "A New Algorithm and System for the Characterization of Handwriting Strokes with Delta-Lognormal Parameters", *IEEE Transactions on Pattern Analysis and Machine Intelligence*, vol.31, no.11, pp.2060-2072, Nov. 2009.

Miguel A. Ferrer received the M.Sc. degree in telecommunications, in 1988, and his Ph.D. degree, in 1994, each from the Universidad Politécnica de Madrid, Spain. He belongs to the Digital Signal Processing research group (GPDS) of the research institute for technological development and Communication Innovation (IDeTIC) at the University of Las Palmas de Gran Canaria in Spain where since 1990 he has been an Associate Professor. His research interests lies in the fields of computer vision, pattern recognition, biometrics, mainly those based on hand and handwriting, audio quality, mainly for health and condition machinery evaluation and vision applications to fisheries and aquaculture.

Moises Diaz-Cabrera received two M. Tech degrees in 2010: Industrial Engineering and Industrial Electronics and Automation Engineering and holds a M.Sc. in Intelligent Systems and Numerical Applications in Engineering (2011) as well as a M.Ed. in Secondary Education (2013), all from La Universidad de Las Palmas de Gran Canaria. He is currently pursuing a Ph.D. degree and his research areas include handwritten signature recognition, pattern recognition and computer vision. He has been a visiting student researcher at the University of Bary, Italy. Also he has some experience in Intelligent Transportation Systems through collaborations with CICEI, at ULPGC, and VI slab, at the University of Parma.

Aythami Morales received his M.Sc. degree in Telecommunication Engineering in 2006 from Universidad de Las Palmas de Gran Canaria. He received his Ph.D degree from La Universidad de Las Palmas de Gran Canaria in 2011. He performs his research works in the Digital Signal Processing Group (GPDS) at Las Palmas de Gran Canaria University and he has undertaken research visits to the Biometric Research Laboratory at Michigan State University, the Biometric Research Center at Hong Kong Polytechnic University and the Biometric System Laboratory at University of Bologna. His research interests are focused on pattern recognition, computer vision, machine learning and biometrics signal processing. He is the author of more than 30 scientific articles published in international journals and conferences.